Journal of Power Sources 255 (2014) 404–409

Contents lists available at ScienceDirect

Journal of Power Sources

journal homepage: www.elsevier.com/locate/jpowsour

Carbon-tolerant solid oxide fuel cells using $NiTiO_3$ as an anode internal reforming layer

Zhiquan Wang [a], Zhenbin Wang [a], Wenqiang Yang [a], Ranran Peng [a,*], Yalin Lu [b,a,1]

[a] CAS Key Laboratory of Materials for Energy Conversion, Department of Materials Science and Engineering, University of Science and Technology of China, Hefei, 230026 Anhui, China

[b] Hefei National Laboratory of Physical Science at the Microscale, University of Science and Technology of China, Hefei, 230026 Anhui, China

HIGHLIGHTS

- $NiTiO_3$ reforming layer could effectively improve carbon tolerance of SOFCs.
- $NiTiO_3$ could be reduced into nickel metal and rutile.
- $NiTiO_3$ reforming layer benefits fuel oxidation reaction.

ARTICLE INFO

Article history:
Received 30 October 2013
Received in revised form
3 January 2014
Accepted 4 January 2014
Available online 15 January 2014

Keywords:
Internal reforming layer
Carbon tolerant
Solid oxide fuel cells
Hydrocarbon fuels

ABSTRACT

In this work, adding a $NiTiO_3$ (NTO) reforming layer is firstly adopted as a low cost method to improve the carbon tolerance in solid oxide fuel cells. XRD patterns suggest that NTO has a good chemical compatibility with the YSZ electrolyte, and NTO can be totally reduced to Ni and TiO_2 when exposing to the H_2 atmosphere. Maximum power densities for the cells with the NTO layers at 700 °C are 270 $mWcm^{-2}$ with wet H_2 fuel, and 236 $mWcm^{-2}$ with wet methane fuel, respectively. Improved discharging stability for the cells with NTO layers has also been observed. The current density remains unchanged for the cells with NTO layers during a 26 h test, while it drops to zero within 1 h for the cells without NTO. Above electroperformance and long term stability tests suggest that fabricating a NTO reforming layer on the anode surface is an efficient and inexpensive method to realize highly carbon tolerant SOFCs.

1. Introduction

The ability to adapt to multiple hydrocarbon fuels is one of the most promising properties that make solid oxide fuel cells (SOFCs) theoretically superior to other types of fuel cells [1]. In practice, typical nickel based anodes of SOFCs have high catalytic activity for the cracking reaction of hydrocarbon fuels, and this usually results in carbon deposition on active sites of nickel and at last in a breakdown of the cells [2,3]. Extensive past efforts have been paid to improve the carbon tolerance of those cells [4], and a few progresses have been achieved mainly as follows: 1) Exploring novel anode materials with low catalytic activity to the hydrocarbon cracking reaction. For instance, this includes Cu metal [5–7] and some conducting ceramics such as $La_{0.75}Sr_{0.25}Cr_{0.5}Mn_{0.5}O_{3-\delta}$ (LSCM) [8,9], doped $SrTiO_3$ (STO) [10,11], $Sr_2Fe_{1.5}Mo_{0.5}O_{6-\delta}$ (SFM) [12], and $Pr_{0.4}Sr_{0.6}Co_{0.2}Fe_{0.7}Nb_{0.1}O_{3-\delta}$ [13]; 2) Modifying the microstructure of Ni based anodes by impregnating CeO_2 [14], or depositing BaO nano-particles onto the anode internal surface to reduce the carbon depositing [15]; and 3) Applying an internal reforming layer onto the anode surface to modify the fuel compositions before following to the anode, such as Ru–CeO_2 [16] and $Cu_{1.3}Mn_{1.7}O_4$ [17] reforming layers. Yet, challenges still exist if to develop a commercial carbon tolerant SOFC with low cost and easy fabrication. For example, Cu and ceramic anodes present low catalytic activity to the oxidation reaction of fuels, and unfortunately, depress the cell discharging performance. Moreover, application of the mainly rare-earth-element composed ceramic anodes, noble metal or the impregnation usually leads to a high material cost and a fabrication cost too, which hinders the commercial process of such SOFCs.

TiO_2 has been widely applied as a low cost and efficient catalyst or catalyst support for the oxidation and the steam reforming of hydrocarbons, including CO [18], methane [19,20], propane [21], methanol [22], glycerol [23] and so on. It's generally accepted that

* Corresponding author. Tel./fax: +86 551 63600594.
E-mail addresses: pengrr@ustc.edu.cn (R. Peng), yllu@ustc.edu.cn (Y. Lu).
[1] Tel./fax: +86 551 63603004.

0378-7753/$ – see front matter © 2014 Elsevier B.V. All rights reserved.
http://dx.doi.org/10.1016/j.jpowsour.2014.01.014

large amounts of oxygen vacancies over TiO_2 surface in reducing atmosphere help to adsorb steam and thus provide oxygen species for the oxidation or reforming of hydrocarbons [24–26]. Shinde et al. [20] prepared 15% Ni/TiO_2 catalyst for methane steam reforming, and found that 92% CH_4 conversion and 77% CO selectivity was observed under a H_2O/CH_4 ratio of 1.2 at 700 °C. Especially, the Ni/TiO_2 catalyst is coke resistant at low steam/carbon ratios.

In this work, inexpensive $NiTiO_3$ (NTO) was firstly used in SOFCs as a novel anode reforming layer in order to improve the carbon tolerance of Ni–YSZ anodes. In a reducing atmosphere, NTO decomposed to Ni and TiO_2, which facilitated the water reforming reaction of hydrocarbon fuels. Fueled with methane and propane, discharging performance and stability of the cell have been significantly enhanced when applying the NTO reforming layer to the cells.

2. Experiment

2.1. Powders synthesis

$NiTiO_3$ (NTO) powders were prepared through a citric acid-nitrate combustion method. Tetrabutyl titanate (analytical grade) was dissolved in dilute nitric acid under stirring, and then nickel nitrate was put into the solution in a stoichiometric ratio. Citric acid and ethylenediamine tetraacetic acid (EDTA) were added to the solution as reducing and complexing agent. Molar ratio of total metal ions: citric acid: EDTA was set at 1:1:1.5. Ammonia was dropped to the solution to adjust the pH value to approximately 6.8. Dry foam was formed when heating such precursor on a heat plate and crystallized NTO powders were prepared after calcining the foam at 950 °C for 2 h. $Y_{0.15}Zr_{0.85}O_{1.93}$ (YSZ) [27], $La_{0.8}Sr_{0.2}MnO_{3-\delta}$ (LSM) [28] and NiO [29] powders were all synthesized by a glycine nitrate process, as reported previously.

2.2. Fabrication of the single cells

Dip-coating method was applied to deposit thin YSZ film on the porous NiO–YSZ anode substrate. The fabrication process details were as follows: 1) NiO, YSZ and graphite mixtures were cold pressed into pellets and then pre-sintered at 800 °C for 2 h as anode substrate; 2) Suspension consisted of YSZ powders and some organic agents was dropped onto the anode surface. After drying at room temperature, the samples were co-sintered at 1350 °C for 5 h to obtain a dense electrolyte film; 3) Slurry containing LSM and YSZ powders (1:1 in weight ratio) was printed on the electrolyte surface, and then fired at 1100 °C for 2 h to complete the fabrication process for a cell with NiO–YSZ|YSZ|LSM–YSZ structure.

Fabrication procedure for the NTO reforming layer is similar to that for the cathode layer. NTO powders were mixed with ethocel, and abietyl alcohol as printing slurry, and then applied onto the anode surface to form a thin layer. After drying, the samples were fired at 1100 °C for 2 h to complete the fabrication process.

2.3. Characterizations

To investigate their chemical compatibility, a mixture consisting of NTO and YSZ powders (1:1 in weight ratio) was cold-pressed into a pellet and then fired at 1100 °C for 2 h. X-ray diffraction (XRD) analysis was performed to investigate the crystalline structure of the sintered samples using a Philips X'pert PROS diffractometer with Cu-K_α radiation at room temperature. X-ray diffraction patterns of NTO powders before and after reducing at 750 °C in H_2 atmosphere for 2 h were also investigated.

Electrochemical performance of the single cells with and without the NTO reforming layer was investigated from 550 °C to 800 °C in a home-developed-cell-testing system using a Zahner Im6e electrochemical workstation. Humidified (~3% H_2O) hydrogen, methane or propane was used as the fuel and ambient air as the oxidant. Impedance spectra of single cells were carried out to investigate the area specific resistance of single cells using Im6e electrochemical workstation in a frequency range of 1 MHz–100 mHz with an ac perturbation signal of 10 mV. Long term performance of single cells with and without the NTO reforming layer was characterized at 0.6 V fueled with humidified CH_4 and propane, respectively. The microstructures of post-tested single cells were imaged using a Jeol (JXA-8100) scanning electron microscope (SEM).

3. Results and discussion

Fig. 1 shows the electrochemical performance of single cells with and without the NTO reforming layer when using wet hydrogen as a fuel measured from 700 to 800 °C. The cells with and without NTO layers have similar behaviors on both open circuit voltage and maximum power density, as shown in Fig. 1. The open circuit voltages (OCVs) and the maximum power densities (P_{max}) of the cell with NTO layer are about 1.04 V and 270 mWcm^{-2}, and 1.01 V and 664 mWcm^{-2} measured at 700 and 800 °C, respectively. Values of polarization resistances (R_p, length of the impedance arc) for the cells with NTO layers are approximately 0.38, 0.86 and 1.80 Ωcm^2 measured at 800, 750 and 700 °C, respectively, as shown in Fig. 2.

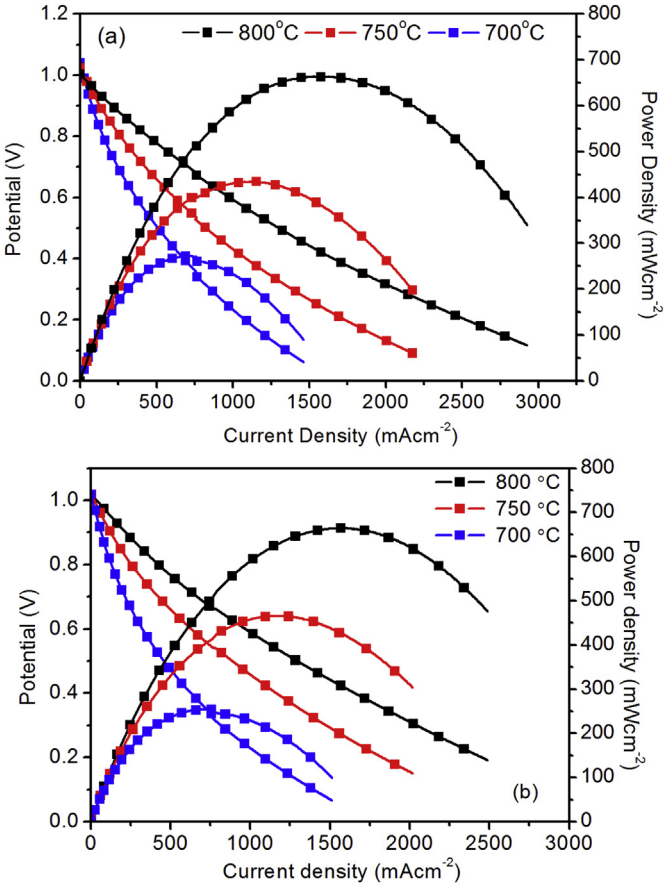

Fig. 1. *I–V* and *I–P* curves of the cells (a) with and (b) without the NTO reforming layer fueled with wet hydrogen.

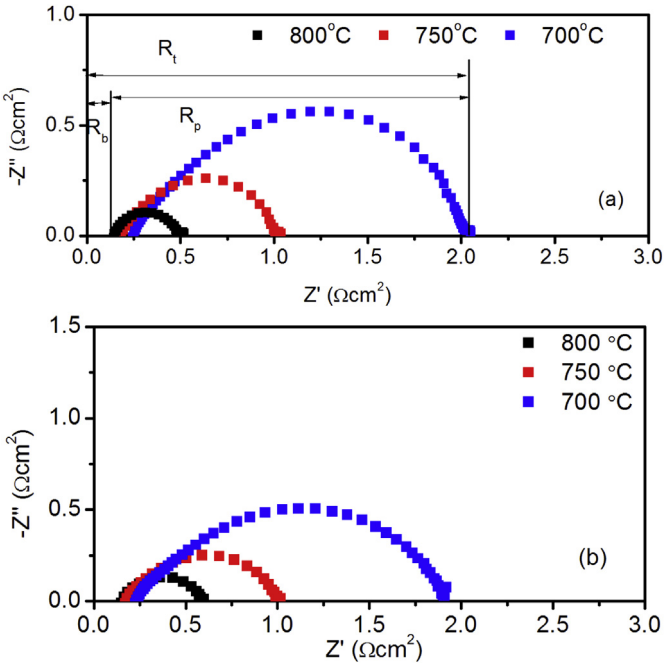

Fig. 2. Impedance spectra of the cells (a) with and (b) without the NTO reforming layer measured under open circuit conditions with wet hydrogen as the fuel.

Fractured microstructures of the cell with the NTO layer are shown in Fig. 3. The NTO layer, approximately 50 μm thick, adheres well to the anode even after the performance test. The XRD pattern, as shown in Fig. 4(c), suggests that NTO (PDF# 33-0960) is totally reduced to Ni (PDF# 04-0850) and rutile TiO_2 (PDF# 21-1276) mixture after exposing to the hydrogen atmosphere. And therefore, Ni and TiO_2 should be the actual materials accounting for the enhanced anode performance for cells with NTO layers. When comparing the XRD patterns in Fig. 4(a) and (b), we can also conclude that NTO and YSZ have good chemical compatibilities at the fabrication temperature (1100 °C) for the NTO layer.

Fueled with humidified methane, *I–V* curves and the impedance spectra of the cell without the NTO layer are shown in Fig. 5. OCV of the cell in wet methane fuel is 0.97 V, approximately 0.07 V lower than that in wet hydrogen fuel. Moreover, the polarization resistance (as shown in Fig. 5) of the cell unfavorably expanded to

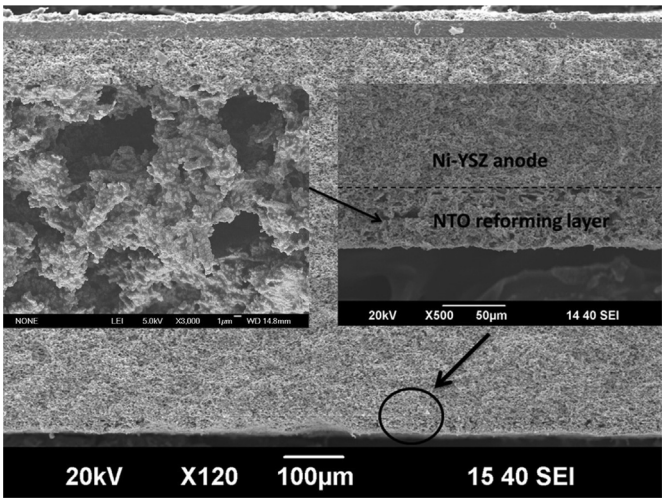

Fig. 3. The fracture microstructures of the cell with the NTO layer after testing.

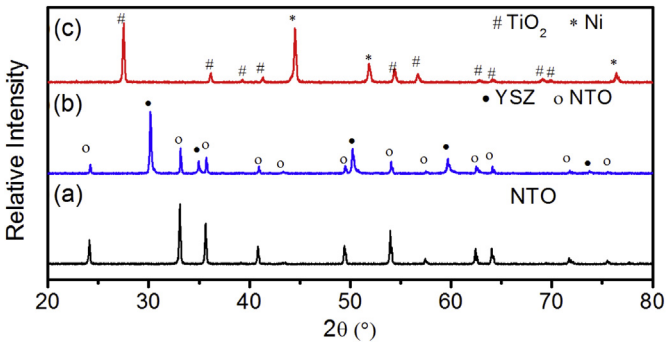

Fig. 4. XRD patterns of (a) NTO powders calcined at 900 °C for 2 h in air, (b) NTO–YSZ mixtures (1:1 in weight ratio) co-fired at 1100 °C for 2 h, and (c) NTO powders reduced in H_2 at 750 °C for 5 h.

3.83 Ωcm^2, almost twice of that fueled with hydrogen (1.92 Ωcm^2). The maximum power density of the cell without the NTO layer is 146 mWcm^{-2} at 700 °C with wet methane fuel, only 56% of that with hydrogen fuel.

While for the cell with the NTO layer, the electro-performance with methane fuel have been significantly improved compared with that without the NTO layer. As shown in Fig. 6(a) and (b), The OCV is 1.03 V, similar to that in humidified hydrogen. Especially, the polarization resistance of the cell with the NTO layer is 2.51 Ωcm^2 in wet methane fuel, much lower than that without the NTO layer. These good performances should come from the accelerated methane steam reforming reaction by the formed nano Ni and TiO_2 particles in reforming layer in the reducing atmosphere, as shown in eq. (1). Especially, large amounts of oxygen vacancies on TiO_2 surface could efficiently upshift the reforming reaction ratio when

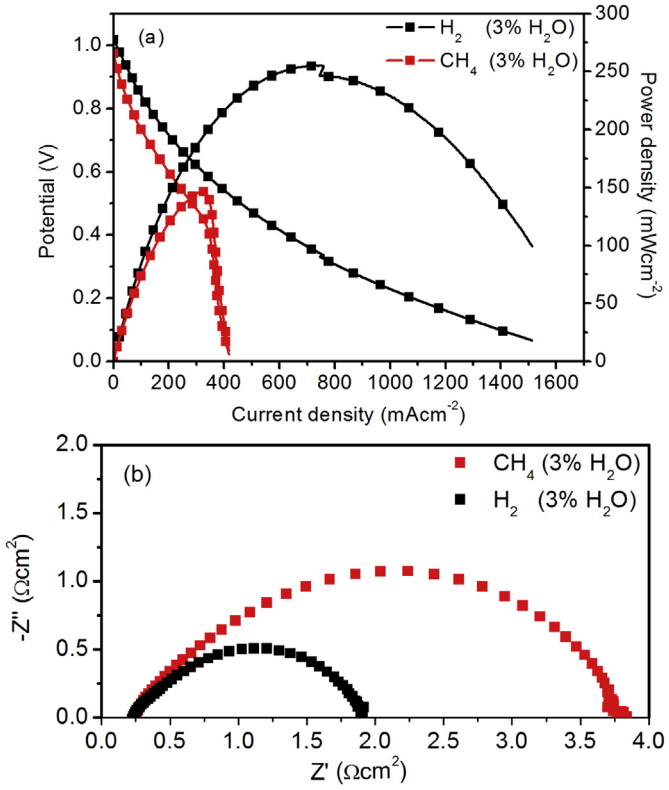

Fig. 5. (a) *I–V* and *I–P* curves and (b) impedance spectra of the cell without the NTO layer measured at 700 °C with wet hydrogen and methane as the fuels, respectively.

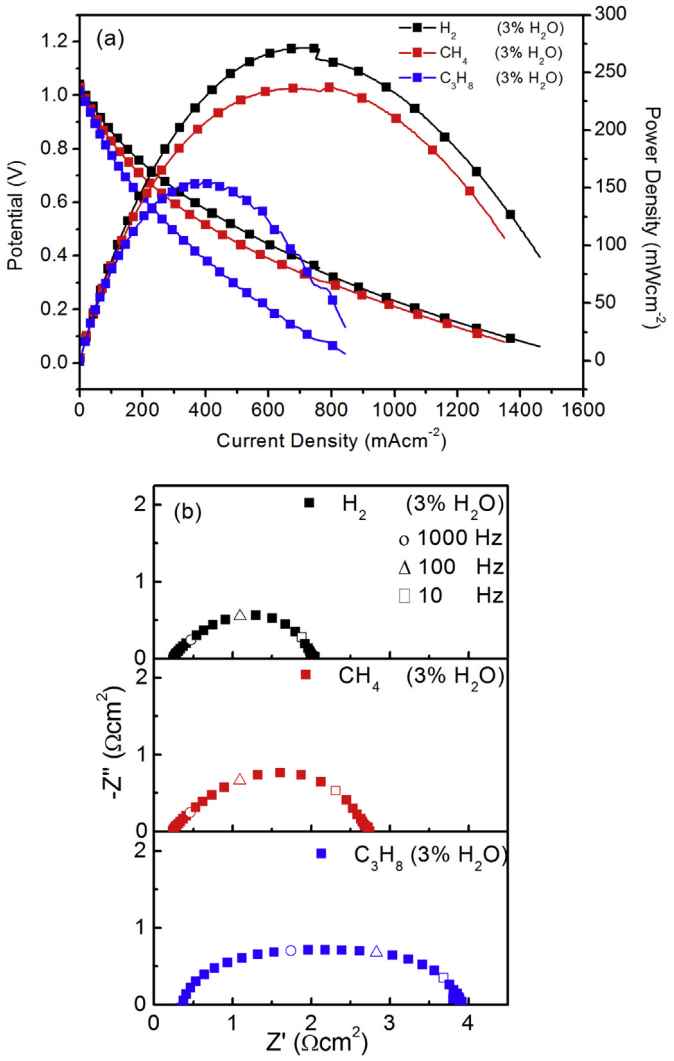

Fig. 6. (a) *I–V* and *I–P* curves and (b) the corresponding impedance spectra of the cell with the NTO layer fueled by wet H_2 (■), CH_4 (■), and C_3H_8 (■), respectively, measured at 700 °C.

used as the catalysts support [30–33]. Fueled with methane, the cell with the NTO layer show a maximum power density of 236 mWcm^{-2} at 700 °C.

$$CH_4 + H_2O{=}CO + 3H_2 \quad (1)$$

I–V curve and impedance spectrum of the cell with NTO fueled with wet propane are also shown in Fig. 6. Compared with those fueled with methane and hydrogen, the cell with wet propane fuel has relatively lower electro-performance, and its maximum power density and polarization resistance are 153 mWcm^{-2} and 3.58 Ωcm^2 at 700 °C, respectively. Linear temperature dependence of R_p is observed for the cell with the NTO layer measured with various fuels, as shown in Fig. 7(a) and (b). The activation energies of R_p are 1.23, 0.77 and 1.50 eV fueled with humidified hydrogen, methane and propane, respectively. Large difference in activation energies and polarization resistances should be attributed to the different fuel oxidation reactions in anode. Low activation energy of the cell in methane seems to suggest that the methane dynamically prefers to operate at low temperature, while that of propane imply that propane favors a high temperature operation. The maximum powder densities (P_{max}) of cell tested in humidified CH_4 and H_2

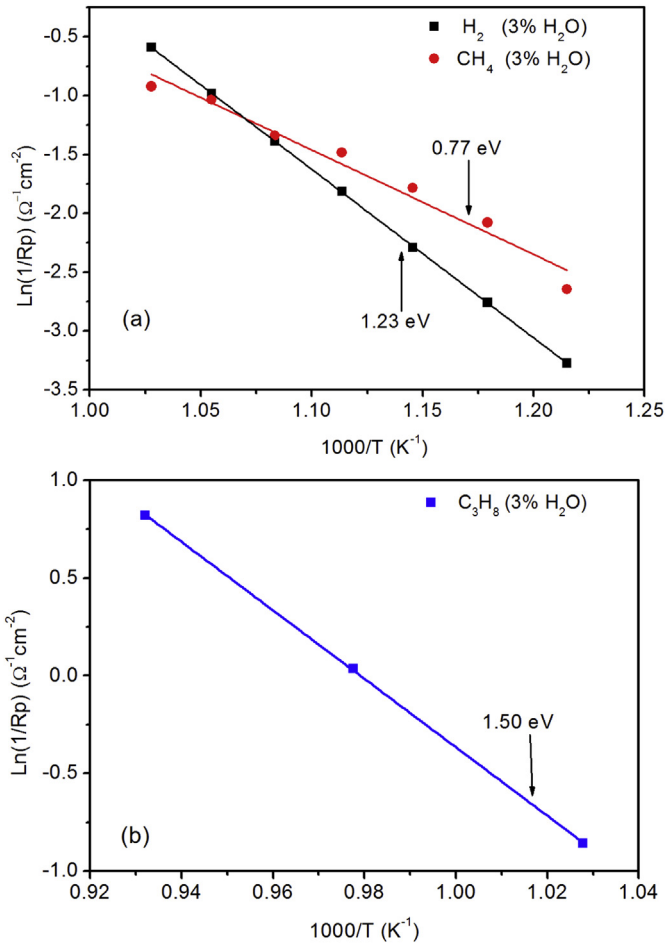

Fig. 7. Temperature dependence of polarization resistances (R_p) for the cell with the NTO layer measured with various fuels.

fuels would support this comment. As shown in Fig. 8(a), the ratio of $P_{max}, CH_4/P_{max}, H_2$ reduces with the temperature when it is below 650 °C. At temperature above 650 °C, the ratio increases with the temperature mainly because of the enhanced OCVs measured at high temperature, as shown in Fig. 8(b).

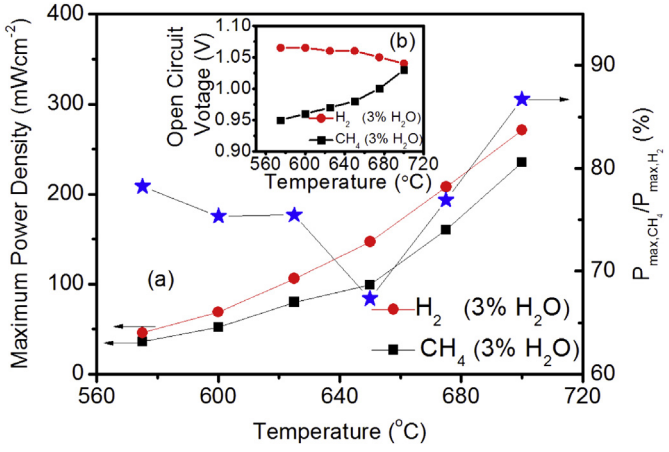

Fig. 8. (a) Temperature dependence of the maximum power densities for the cell with the NTO layer measured in humid H_2 (■) and CH_4 (●) fuels, respectively, and also the temperature dependence of $P_{max}, CH_4/P_{max}, H_2$ (★); and (b) open-circuit voltages for the cell measured in H_2 and CH_4 fuels, respectively.

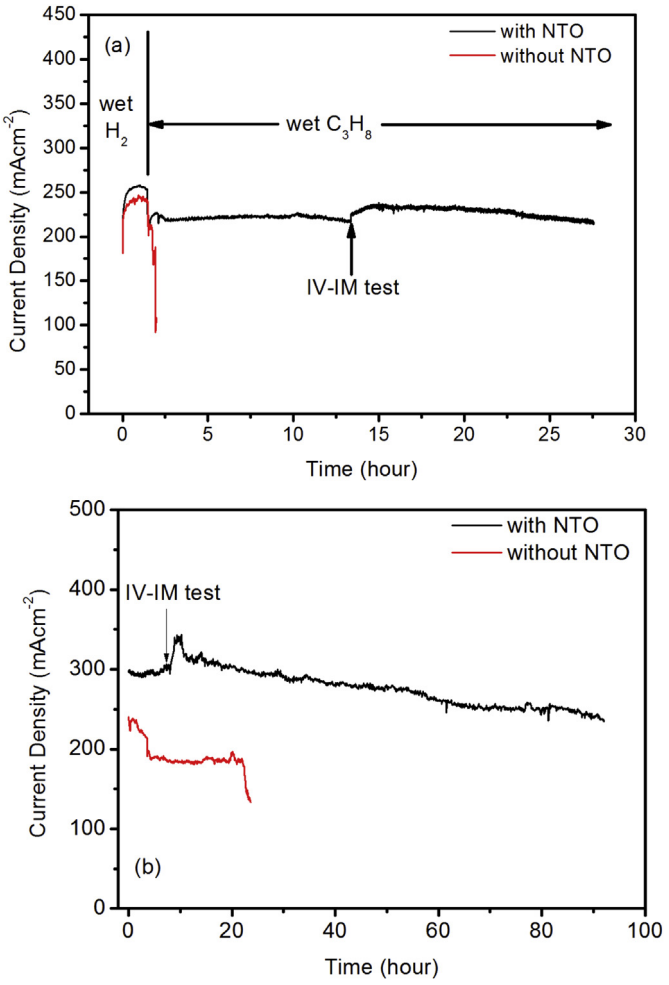

Fig. 9. Current densities of the cell with (black) and without (red) the NTO layer discharging at 0.6 V measured at 700 °C with wet C_3H_8 (a) and CH_4 (b) as fuels. (For interpretation of the references to colour in this figure legend, the reader is referred to the web version of this article.)

Long-time performances of the cells with and without the NTO layer are characterized with humidified methane and propane fuels, respectively, as shown in Fig. 9(a) and (b). Discharging at 0.60 V with propane fuel, no obvious declining in current density is observed for the cell with the NTO layer within the 26 h test, while that for the cell without the NTO layer drops to zero within 1 h. This result highly suggests that the NTO layer could effectively avoid the carbon depositing on the Ni catalyst. Fueled with methane, much improved discharging stability is also achieved for the cell with the NTO layer, as shown in Fig. 9(b). These results strongly suggest that the low-cost NTO reforming layer can effectively improve the carbon tolerance of cells.

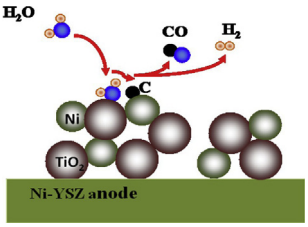

Fig. 11. Schematic diagram for carbon extinguishment within the Ni–TiO_2 reforming layer.

SEM pictures of the cell after running in humidified methane for 93 h are shown in Fig. 10. It can be clearly seen that slight carbon deposits on Ni–YSZ anode while none on the Ni–TiO_2 reforming layer is observed for the cell with the NTO layer after the long term test. Small amount of methane, sneaking out of the reforming layer to the Ni/YSZ anode, catalytically cracked to carbon on Ni particles, and therefore resulted in slight decrease of current density for cells.

The mechanism for the much improved carbon tolerance of the cell with the NTO layer can be suggested as follows. In a reducing atmosphere, the NTO layer decomposed to Ni and TiO_2 particles. Especially, Ti^{4+} in TiO_2 would be intensively reduced to Ti^{3+} which led to large amounts of oxygen vacancy defects on the surface. Aschauer et al. investigated the water adsorption on reduced TiO_2 and suggested that the TiO_2 surface containing oxygen vacancies show a strong selective adsorption to H_2O even at high temperatures [25]. Fig. 11 gives a schematic diagram for the reforming reaction within the NTO layer: 1) the NTO layer decomposed to Ni and TiO_2 particles; 2) water vapor selectively adsorbed on the reduced TiO_2 surface; 3) the adsorbed water reacts with the carbon depositing on the neighboring Ni particles to generate CO and H_2. After those, CO and H_2 gases will pass through Ni–YSZ anode and intensively react with O^{2-} transferring from the cathode to generate H_2O and CO_2.

4. Conclusion

For the first time, $NiTiO_3$ (NTO) was employed as the anode reforming layer to ameliorate the carbon tolerance of SOFCs. In the reducing atmosphere, NTO was reduced to nano Ni and TiO_2 particles, which could efficiently accelerate the methane steam

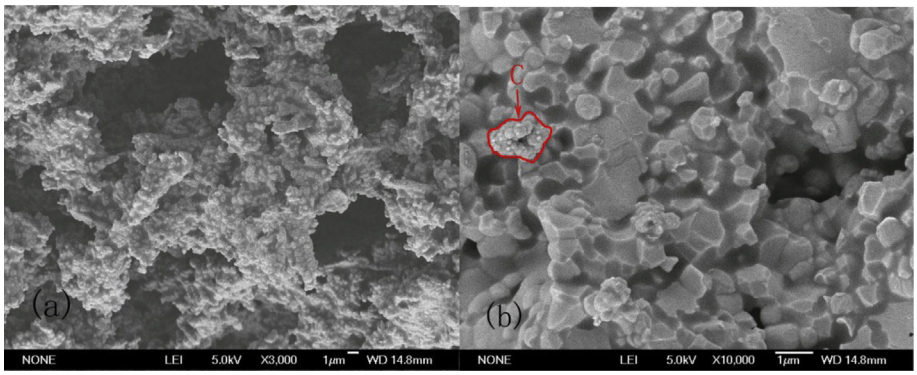

Fig. 10. The fractured SEM pictures of (a) the reforming layer and (b) the Ni–YSZ anode of the cell with NTO layer after tested in methane for 93 h.

reforming reaction. The cell with the NTO reforming layer discharged smoothly in the propane fuel within a 26 h test; while without the NTO layer, it cracked within 1 h. The maximum power densities for the cells with the NTO layer at 700 °C were 270 and 236 $mWcm^{-2}$ with wet hydrogen and wet methane fuels, respectively.

Acknowledgments

This work was financially supported by the Natural Science Foundation of China (51072193), the National Basic Research Program of China (973 Program, 2012CB922001), and the Fundamental Research Funds for the Central Universities.

References

[1] Y. Lin, Z. Zhan, J. Liu, S. Barnett, Solid State Ionics 176 (2005) 1827–1835.
[2] H. He, J.M. Hill, Appl. Catal. A Gen. 317 (2007) 284–292.
[3] N. Galea, D. Knapp, T. Ziegler, J. Catal. 247 (2007) 20–33.
[4] W. Wang, C. Su, Y. Wu, R. Ran, Z. Shao, Chem. Rev. 113 (2013) 8104–8151.
[5] S. Jung, C. Lu, H. He, K. Ahn, R.J. Gorte, J.M. Vohs, J. Power Sources 154 (2006) 42–50.
[6] S. Park, J.M. Vohs, R.J. Gorte, Nature 404 (2000) 265–267.
[7] R.J. Gorte, S. Park, J.M. Vohs, C. Wang, Adv. Mater. 12 (2000) 1465–1469.
[8] S. Tao, J.T. Irvine, Nat. Mater. 2 (2003) 320–323.
[9] S. Tao, J.T.S. Irvine, Chem. Mater. 16 (2004) 4116–4121.
[10] O.A. Marina, N.L. Canfield, J.W. Stevenson, Solid State Ionics 149 (2002) 21–28.
[11] Q. Ma, F. Tietz, Solid State Ionics 225 (2012) 108–112.
[12] Q. Liu, X. Dong, G. Xiao, F. Zhao, F. Chen, Adv. Mater. 22 (2010) 5478–5482.
[13] C. Yang, Z. Yang, C. Jin, G. Xiao, F. Chen, M. Han, Adv. Mater. 24 (2012) 1439–1443.
[14] X.J. Chen, K.A. Khor, S.H. Chan, Electrochem. Solid State Lett. 8 (2005) A79–A82.
[15] L. Yang, Y. Choi, W. Qin, H. Chen, K. Blinn, M. Liu, P. Liu, J. Bai, T.A. Tyson, M. Liu, Nat. Commun. 2 (2011) 357.
[16] Z. Zhan, S.A. Barnett, Science 308 (2005) 844–847.
[17] I.X. Green, W. Tang, M. Neurock, J.T. Yates Jr., Science 333 (2011) 736–739.
[18] Y. Boucouvalas, Z. Zhang, X.E. Verykios, Catal. Lett. 40 (1996) 189–195.
[19] V. Shinde, G. Madras, RSC Adv. 4 (2013) 4817–4826.
[20] W. Turek, J. Strzezik, A. Krowiak, React. Kinet. Mech. Catal. 107 (2012) 115–125.
[21] R. Pérez-Hernández, A.D. Avendaño, E. Rubio, V. Rodríguez-Lugo, Top. Catal. 54 (2011) 572–578.
[22] I. Rossetti, A. Gallo, V. Dal Santo, C.L. Bianchi, V. Nichele, M. Signoretto, E. Finocchio, G. Ramis, A. Di Michele, ChemCatChem 5 (2013) 294–306.
[23] K.-I. Tanaka, M. Shou, H. He, X. Shi, Catal. Lett. 110 (2006) 185–190.
[24] M. Date, M. Haruta, J. Catal. 201 (2001) 221–224.
[25] U. Aschauer, Y. He, H. Cheng, S. Li, U. Diebold, A. Selloni, J. Phys. Chem. C 114 (2010) 1278–1284.
[26] C. Jin, C. Yang, F. Zhao, A. Coffin, F. Chen, Electrochem. Commun. 12 (2010) 1450–1452.
[27] Q. Wang, R. Peng, C. Xia, W. Zhu, H. Wang, Ceram. Int. 34 (2008) 1773–1778.
[28] R. Peng, X. Fan, Z. Jiang, C. Xia, Fuel Cells 6 (2006) 455–459.
[29] Y. Ji, J. Liu, T. He, L. Cong, J. Wang, W. Su, J. Alloys Compd. 353 (2003) 257–262.
[30] A. Tilocca, A. Selloni, J. Phys. Chem. C 116 (2012) 9114–9121.
[31] M.A. Henderson, Langmuir 12 (1996) 5093–5098.
[32] K. Takanabe, K. Nagaoka, K. Nariai, K. Aika, J. Catal. 232 (2005) 268–275.
[33] R. Schaub, P. Thostrup, N. Lopez, E. Lægsgaard, I. Stensgaard, J.K. Nørskov, F. Besenbacher, Phys. Rev. Lett. 87 (2001) 266104.